



JOURNAL OF
SYNCHROTRON
RADIATION

Volume 26 (2019)

Supporting information for article:

Reactions of $\text{Rh}_2(\text{CH}_3\text{COO})_4$ with thiols and thiolates: a structural study

Alejandra Enriquez Garcia, Farideh Jalilehvand and Pantea Niksirat

Molecular orbital diagram for $\text{Rh}_2(\text{AcO})_4$

Early electronic structure calculations on dirhodium(II) tetraacetate, $\text{Rh}_2(\text{AcO})_4$, using the SCF-Xa-SW method revealed that out of all the metal-centered molecular orbitals (MOs), only the σ^* orbital remains empty and the rest (σ , π , δ , δ^* and π^*) are fully occupied, giving rise to a Rh-Rh bond order of 1.0 (Norman, J. G. & Kolari, H. J., 1978). Despite the common expectation, Norman et al. showed that δ^* is the highest occupied molecular orbital (HOMO) with higher energy than the π^* orbitals; see Figure S1a.

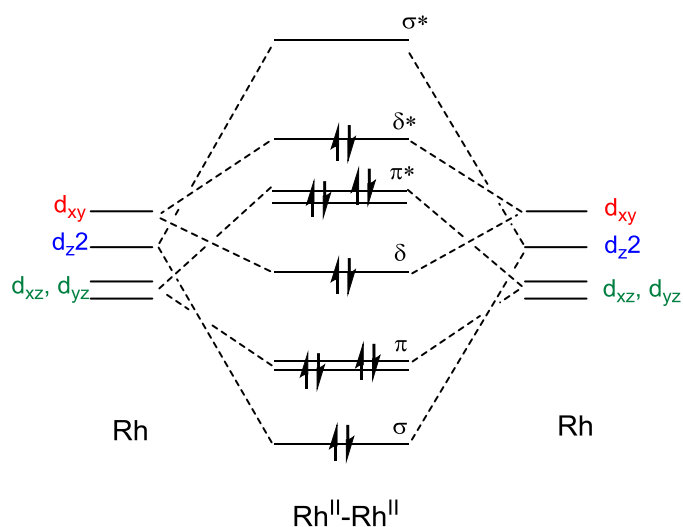


Figure S1a. MO diagram for the dirhodium(II) core in $\text{Rh}_2(\text{AcO})_4$ (Norman, J. G. & Kolari, H. J., 1978)

We observed the same phenomenon when performing the ground state optimization with our selected functional and basis sets (see Figure S1b). The starting geometry for the ground state optimization was obtained using the coordinates of the crystal structure of the aqua complex $[\text{Rh}_2(\text{AcO})_4(\text{H}_2\text{O})_2]$ (Cotton, F. A., 1971), with the axial water molecules removed. Introduction of two axial water molecules causes a shift of the Rh-Rh σ and σ^* orbitals to higher energy (Norman, J. G. & Kolari, H. J., 1978). We made a similar observation using the BHandHLYP functional with our chosen basis sets (see Figure S2a).

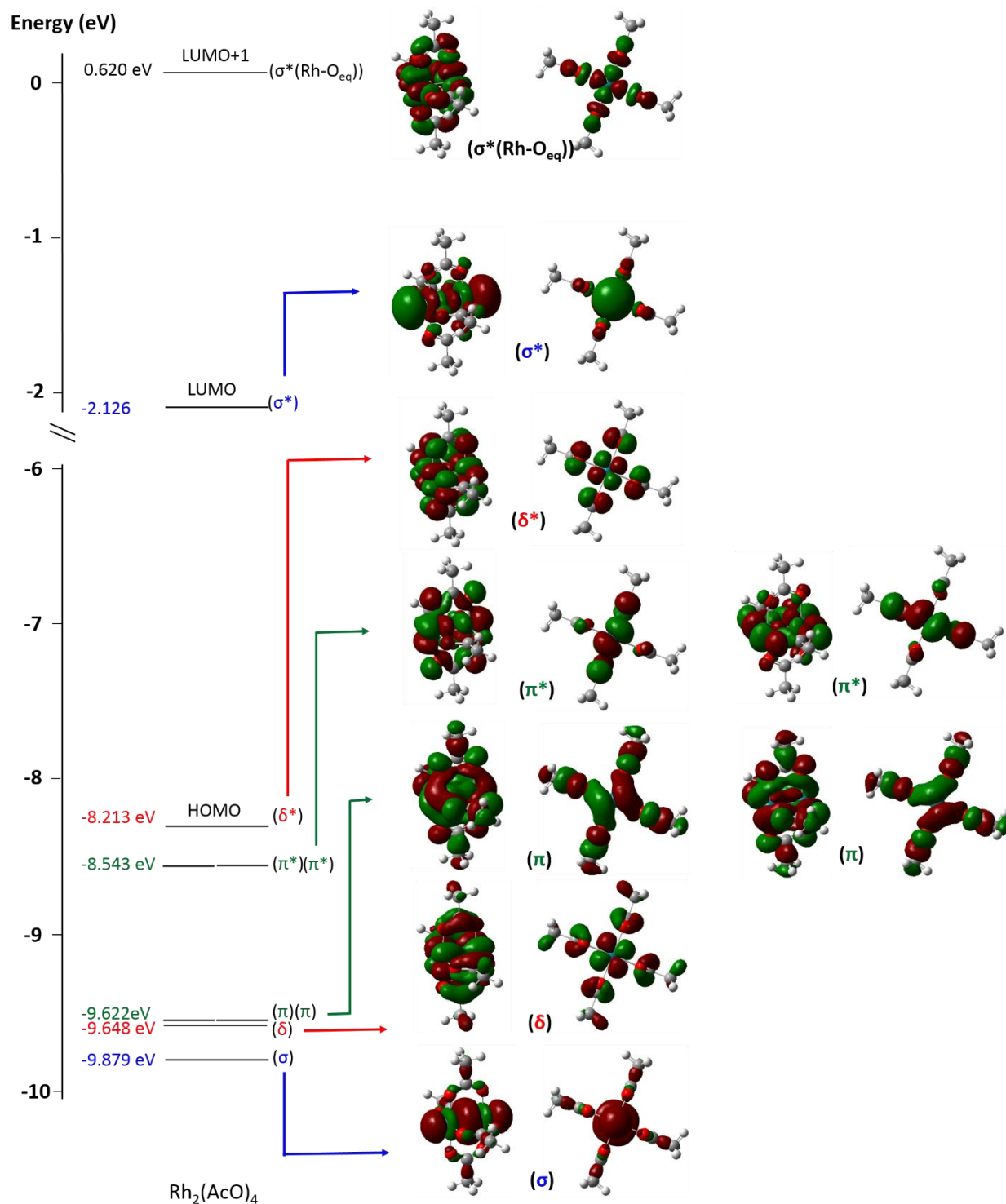


Figure S1b. DFT calculated molecular orbital (MO) diagram and MO energy levels of Rh₂(AcO)₄ in the ground state. MO contours were visualized using the isovalue 0.02.

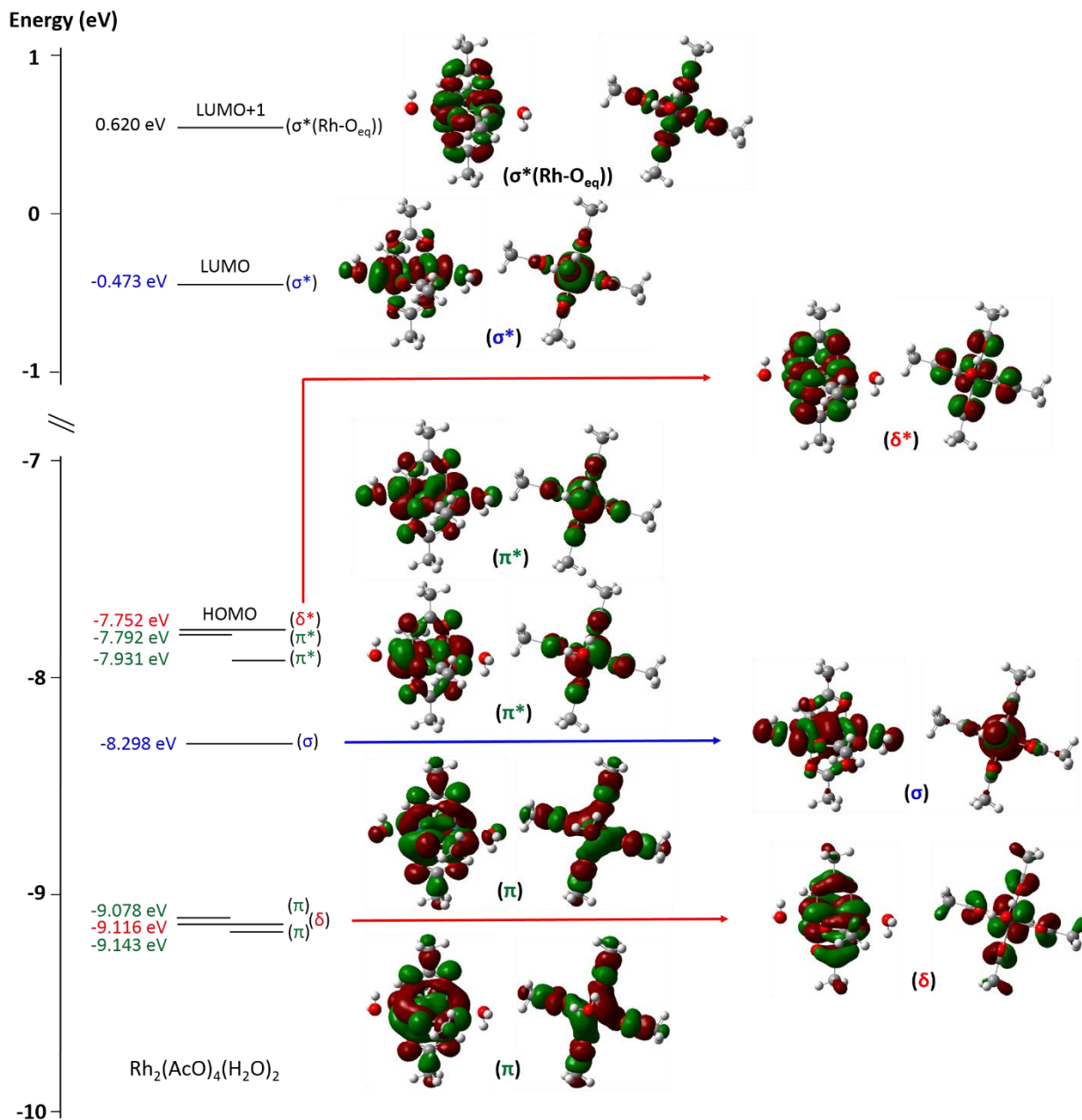


Figure S2a. DFT calculated MO diagram and MO energies of $[\text{Rh}_2(\text{AcO})_4(\text{H}_2\text{O})_2]$ involved in the vertical transitions that give rise to the UV-vis. bands described in Table S1. MO contours were visualized using the isovalue 0.02.

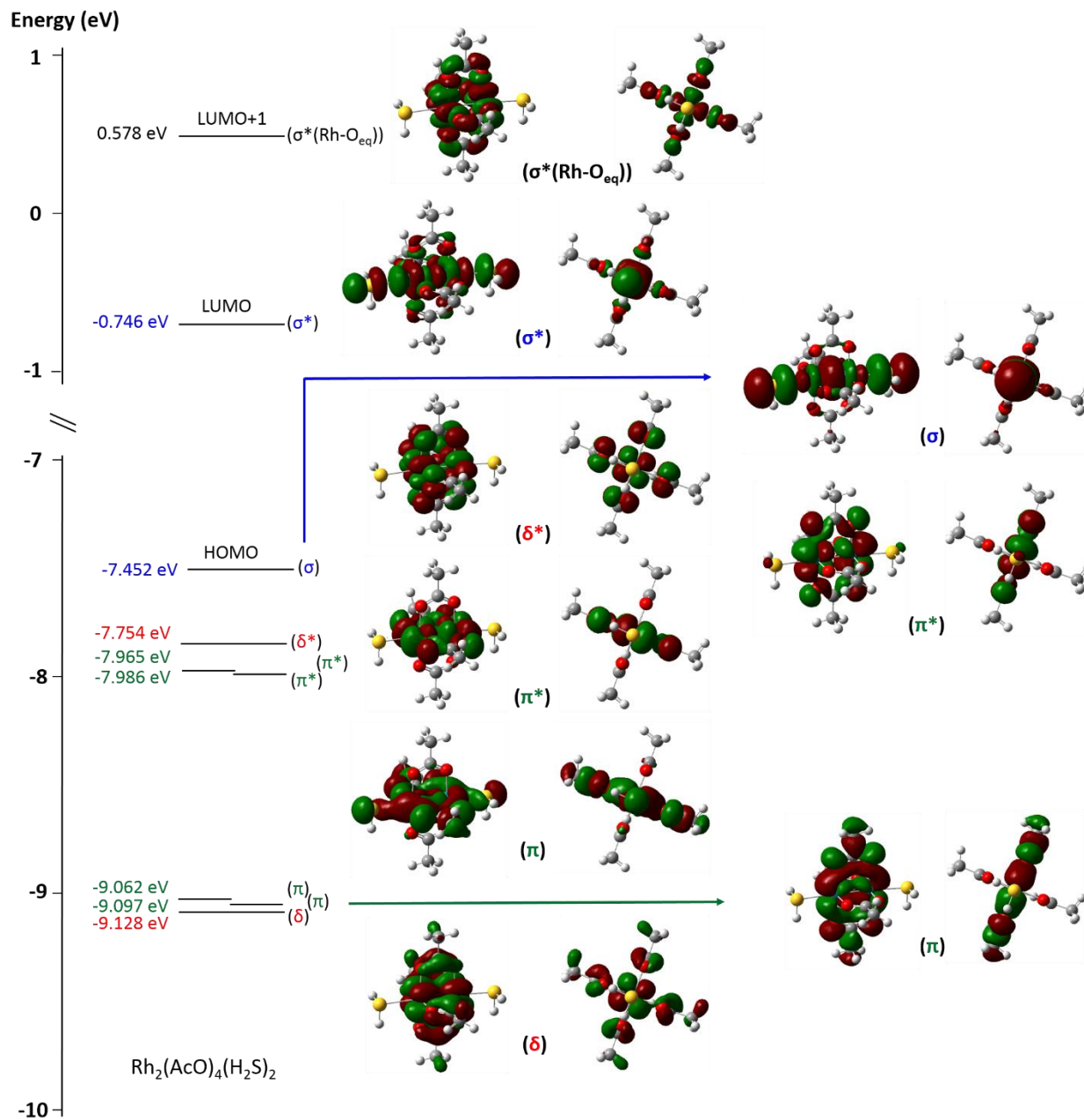


Figure S2b. DFT calculated MO diagram with MO energies of $[\text{Rh}_2(\text{AcO})_4(\text{H}_2\text{S})_2]$. MO contours were visualized using the isovalue 0.02.

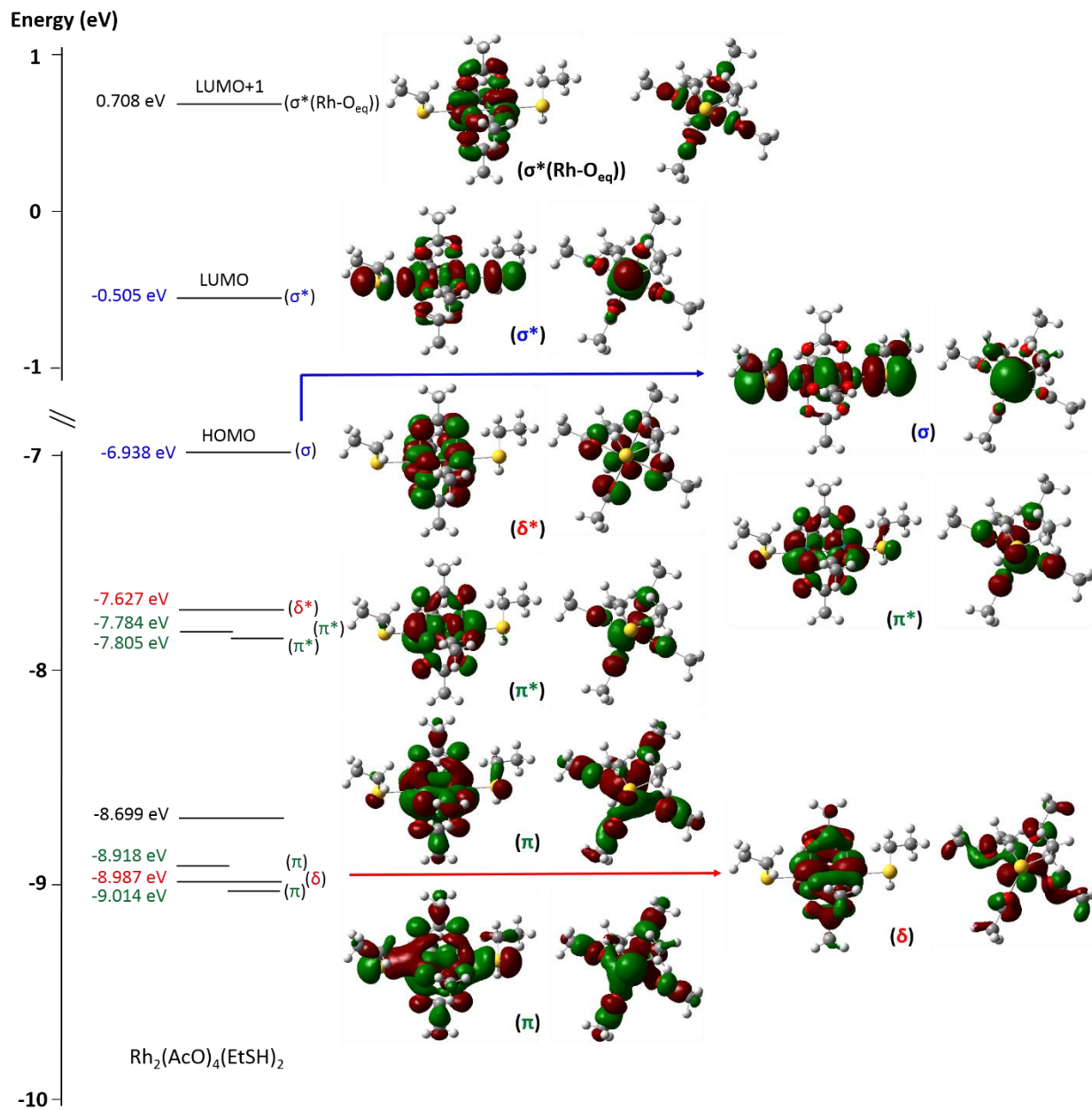


Figure S2c. DFT calculated MO diagram with MO energies of $[\text{Rh}_2(\text{AcO})_4(\text{EtSH})_2]$. MO contours were visualized using the isovalue 0.02.

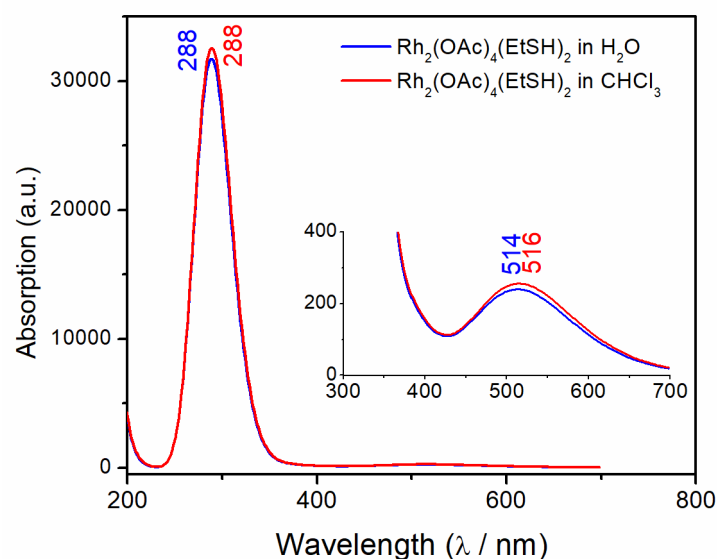


Figure S3. Simulated UV-vis spectra for $[\text{Rh}_2(\text{AcO})_4(\text{EtSH})_2]$ in solvent cavities, surrounding the complex with water and chloroform in the Polarizable Continuum Model (PCM) of the Gaussian 09 package (Frisch *et al.*, 2016).

Table S1. Simulated MO Transitions Between 200-800 nm for $[\text{Rh}_2(\text{AcO})_4(\text{H}_2\text{O})_2]$ and Their Corresponding Expected Absorption Wavelength based on TD-DFT Calculations.

Simulated Absorption Wavelength (nm)	Experimental * Absorption Wavelength (nm)	MO Transition	Transition
541	584	$\pi^* (\text{Rh}_2^{4+}) \rightarrow \sigma^* (\text{Rh}_2^{4+})$	HOMO-1/HOMO-2 \rightarrow LUMO
371	449	$\pi^* (\text{Rh}_2^{4+}) \rightarrow \sigma^* (\text{Rh-O}_{\text{equatorial}})$	HOMO-1/HOMO-2 \rightarrow LUMO+1
239	247	$\sigma (\text{Rh}_2^{4+}) \rightarrow \sigma^* (\text{Rh}_2^{4+})$	HOMO-3 \rightarrow LUMO

* The experimental UV-vis spectrum of $[\text{Rh}_2(\text{AcO})_4(\text{H}_2\text{O})_2]$ is shown in Figure 1.

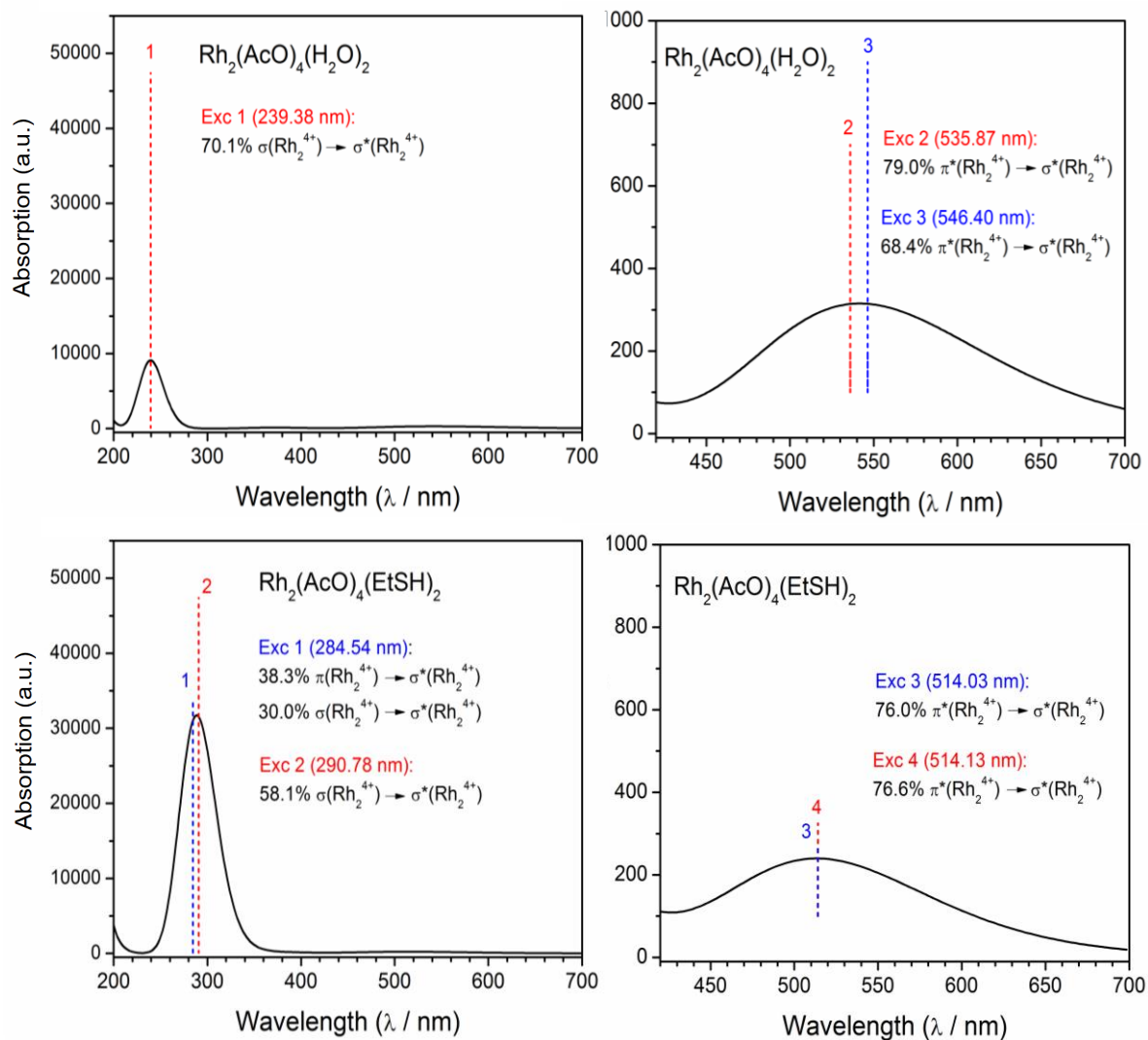


Figure S4. The main excitations in the 200 – 350 nm and 400 – 700 nm regions in the simulated UV-vis. spectra of $[\text{Rh}_2(\text{AcO})_4(\text{H}_2\text{O})_2]$ and $[\text{Rh}_2(\text{AcO})_4(\text{EtSH})_2]$ in water. The vertical transitions with significant contributions ($\geq 10\%$) in each excitation are indicated

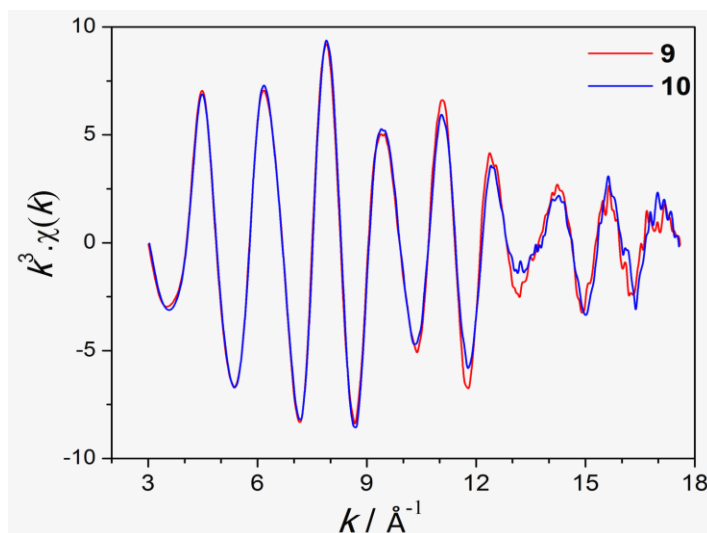


Figure S5. Superimposed k^3 -weighted Rh K-edge EXAFS spectra of the solid reaction products (**9** and **10**) of $\text{Rh}_2(\text{AcO})_4$ with excess of sodium ethanethiolate NaEtS (compound **9**), and of the sodium salt of DHLA (compound **10**).

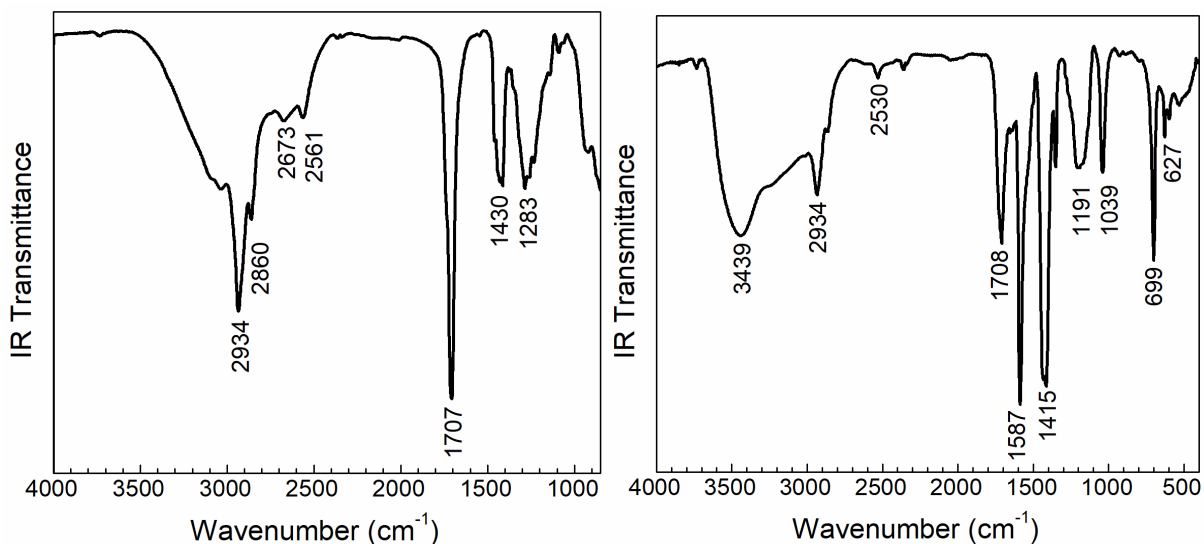


Figure S6. Baseline corrected FT-IR spectra of: (*left*) pure DHLA (oil) held between BaF_2 windows (cut-off 870 cm^{-1}); (*right*) solid $[\text{Rh}_2(\text{AcO})_4(\text{DHLA})]_n$ (**8**) mixed with KBr, measured using a Thermo Nicolet NEXUS 470 FT-IR ESP spectrometer.

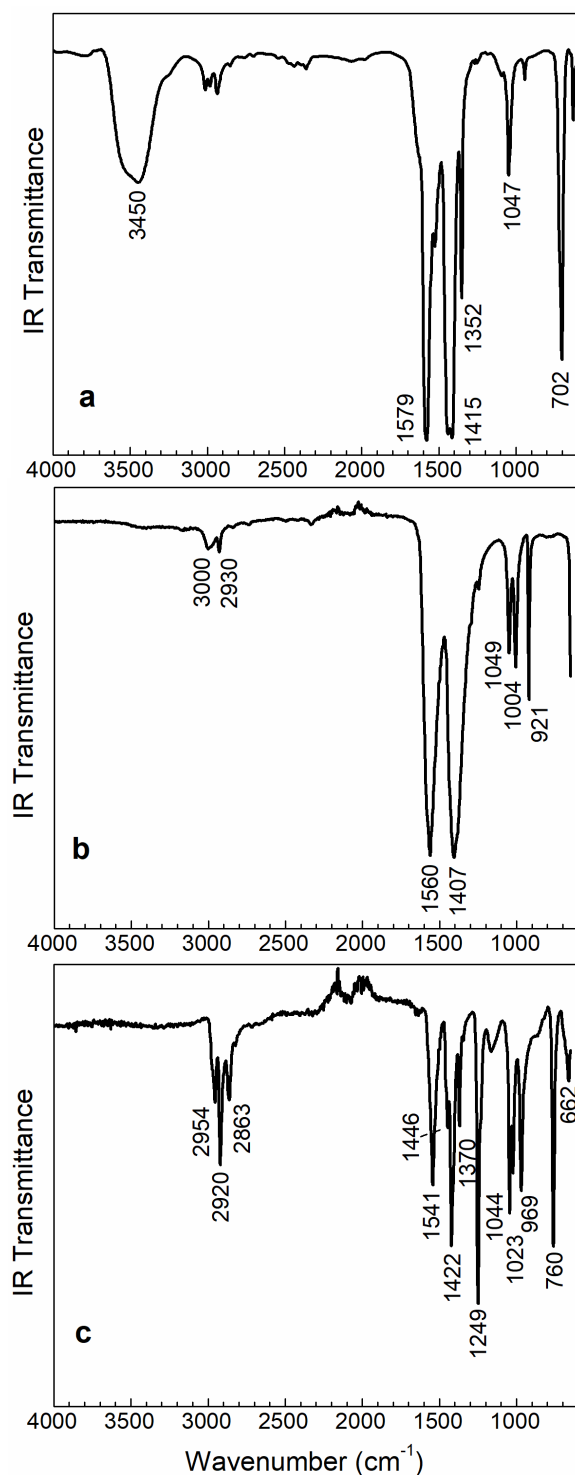


Figure S7. FT-IR spectra of solids: *a*) $\text{Rh}_2(\text{AcO})_4$ (mixed with KBr), *b*) $\text{Na}(\text{AcO})$, and *c*) the reaction product of $\text{Rh}_2(\text{AcO})_4$ with excess amount of sodium ethanethiolate NaEtS (compound **9**). The spectra of $\text{Na}(\text{AcO})$ and **9** were measured using an Agilent Cary 630 FT-IR instrument with a diamond ATR accessory.

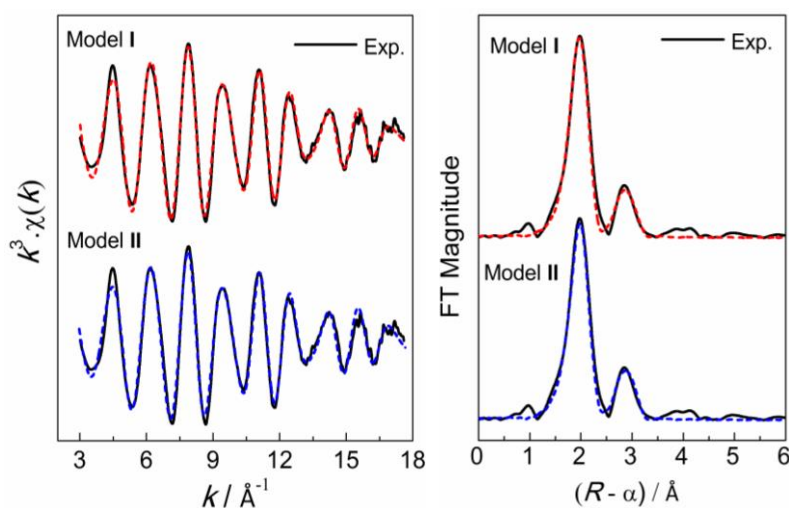
Table S2. Structural Parameters Derived from Least Squares Curve-Fitting of Simulated EXAFS Oscillations (Models **I** – **IV**) to the Experimental EXAFS spectrum of **9**.^a

Model ^b	Rh-O			Rh-S			Rh...Rh			ΔE_0	R ^c
	<i>N</i>	<i>R</i> (Å)	σ^2 (Å ²)	<i>N</i>	<i>R</i> (Å)	σ^2 (Å ²)	<i>N</i>	<i>R</i> (Å)	σ^2 (Å ²)		
I				6.0	2.37	0.0040	1.5	3.18	0.0045	2.9	17.3
II	1 <i>f</i>	2.18	0.0045	5 <i>f</i>	2.37	0.0033	1.4	3.18	0.0043	3.8	17.7
III	2.0	2.20	0.0083	5 <i>f</i>	2.37	0.0034	1.4	3.18	0.0043	4.4	17.6
IV	2 <i>f</i>	2.21	0.0019	4 <i>f</i>	2.38	0.0027	1.3	3.19	0.0042	6.3	19.9

^a Using Feff files from the $\Delta\Lambda$ -[Rh{Ir(aet)₃]₂]Br₃ structure (CSD: AQUVOX) structure to generate Rh-(N/O) path. The amplitude reduction factor (S_0^2) was fixed at 0.92; *f* = fixed; estimated errors: $R \pm 0.02$ Å; $\sigma^2 \pm 0.001$ Å²; $N \pm 10$ -15%; ^b Please note that Model **I** data here are slightly different with those presented for **9** in Table 1, since the multiple-scattering path Rh-S-Rh-S ($n_{\text{leg}} = 4$) could not be implemented here (it is only possible when using the FEFF files from the optimized geometry of [Rh₄(EtS)₁₅]³⁻); Model **III**: very high σ^2 value for Rh-O path; Model **IV**: higher fitting residual than the other fitting models. ^c The fitting residual (%) from the least-squares curve fitting is defined as:

$$\frac{\sum_{i=1}^N |y_{\text{exp}}(i) - y_{\text{theo}}(i)|}{\sum_{i=1}^N |y_{\text{exp}}(i)|} \times 100$$

where y_{exp} and y_{theo} are experimental and theoretical data points, respectively.

**Figure S8.** Right) Comparison between the k^3 -weighted Rh K-edge EXAFS spectrum of **9** and the simulated EXAFS oscillations for Models **I** and **II**; left) corresponding Fourier-transforms.

FEFF8.10 Input files for simulating the XANES spectrum of $[\text{Rh}_2(\text{AcO})_4(\text{EtSH})_2]$

The best results were obtained using the Hedin-Lundqvist exchange-correlation potential (EXCH 0) for the excited state. A negative (-0.8) broadening value was added to improve the agreement with the experimental data, particularly in the width of the first peak. Increasing the l_{max} value (maximum angular momentum bases) from 3 to 4 for the Rh atoms did not seem to affect the fit.

TITLE RhAcEtSH optimized

PRINT 1 1 1 1 1 1

CONTROL 1 1 1 1 1 1

EDGE K 1.0

SCF 10.0 1

FMS 10.0 1

XANES 8

EXCH 0 0 -0.8

CORR 1.5 0.0

POTENTIALS

0 45 Rh 3 3

1 45 Rh 3 3

2 16 S 2 3

3 8 O 2 3

4 6 C 2 3

5 1 H 2 3

ATOMS

-0.1628898	-2.4135221	-0.4330873	4
-0.2708706	-3.8860503	-0.7212408	4
0.6753981	-0.2623534	2.4977347	4
1.0662504	-0.4727523	3.9349524	4
-0.5998970	-4.0142243	-1.7503133	5
-1.0059927	-4.3454838	-0.0707735	5
0.6935788	-4.3665424	-0.6092055	5
0.2396829	-0.8895135	4.4971414	5
1.3292844	0.4903220	4.3670405	5
1.9361818	-1.1166286	3.9979843	5
-1.2072563	-1.8303337	-0.0459202	3
0.9525109	-1.8721512	-0.6255060	3
-0.5481358	-0.1507525	2.2458117	3
-1.6185450	0.5441216	-1.6707233	3
-1.1634820	0.2068838	0.3086630	0
1.1625293	0.1618669	-0.3297731	1
-0.9434414	2.2306510	0.6075332	3
1.6095440	-0.1879342	1.6587200	3
-0.6840456	0.6331417	-2.5080894	4

1.2153226	2.1871526	0.0225666	3
0.5393540	0.5133860	-2.2595495	3
0.1706583	2.7717538	0.4081760	4
-1.0693865	0.9408440	-3.9287502	4
0.2796171	4.2465551	0.6812728	4
-0.3002152	0.6019860	-4.6118957	5
-2.0240598	0.4861303	-4.1671894	5
-1.1742265	2.0186446	-4.0326178	5
-0.6990314	4.7098064	0.6622694	5
0.7132749	4.3862783	1.6690910	5
0.9398542	4.7120089	-0.0418730	5
3.7381828	0.0994156	-0.9517679	2
-3.7259060	0.1721347	0.9848391	2
-4.3676961	-0.9119475	-0.3360285	4
-4.3546222	-0.2844541	-1.2212557	5
-3.6435595	-1.7033145	-0.4910878	5
-3.6094151	-0.7595606	1.9362086	5
4.0976453	1.0771857	-0.1143179	5
4.2711980	-1.3092053	0.0792028	4
3.7377900	-1.2467814	1.0205775	5
3.8954151	-2.1796727	-0.4489924	5
5.7738950	-1.3837616	0.2728597	4
6.1477810	-0.5111702	0.8032917	5
6.0279243	-2.2634718	0.8612780	5
6.2936356	-1.4481757	-0.6787728	5
-5.7578422	-1.4502350	-0.0554912	4
-6.4717000	-0.6454044	0.0946002	5
-6.0964319	-2.0552698	-0.8945028	5
-5.7669965	-2.0792001	0.8316029	5

END

Input files for simulating the XANES spectrum of $[\text{Rh}_4(\text{EtS})_{15}]^{3-}$

The best results were obtained using the Hedin-Lundqvist exchange-correlation potential (EXCH 0) for the excited state. A negative (-0.8) broadening value was added to improve the agreement with the experimental data, particularly in the width of the first peak. Increasing the l_{max} value (maximum angular momentum bases) from 3 to 4 for the Rh atoms did not seem to affect the fit.

TITLE RhAcEtSNa optimized

PRINT 1 1 1 1 1 1

CONTROL 1 1 1 1 1 1

EDGE K 1.0

SCF 10.0 1

FMS 10.0 1

XANES 8

EXCH 0 0 -0.8

CORR 1.5 0.0

POTENTIALS

0 45 Rh 3 3
1 45 Rh 3 3
2 16 S 2 3
3 6 C 2 3
4 1 H 2 3

ATOMS

-1.6606042	0.0118183	-0.1646303	0
-6.4452483	-0.4643212	-1.9479463	2
-6.2555686	2.1550628	0.1514295	2
-6.4148327	-1.1143614	1.4131432	2
4.9782521	-0.1120161	0.1517382	1
1.6644584	-0.0603344	-0.1336234	1
-4.9995534	0.1131607	-0.1097142	1
3.2538298	-1.9047816	-0.1682995	2
-0.0163793	-0.6188292	-1.8795166	2
-0.0430421	-1.1700839	1.2312581	2
3.4018993	0.8909564	-1.560646	2
3.133737	0.5032463	1.6982476	2
0.0317494	1.7770407	0.0917744	2
-3.3191209	-1.7308342	-0.4525464	2
-3.2317996	0.6603302	1.57465	2
-3.2876502	1.3063041	-1.4424769	2
6.2338624	-1.1425788	1.9316967	2
6.3462674	1.8327727	0.570461	2
6.4622304	-0.8927411	-1.5863526	2
3.4427786	-2.5092696	-1.8785467	3
3.9440272	-1.7551299	-2.4730436	4

8.1224076	-1.1134469	-0.8747392	3
8.0975347	-1.9030719	-0.1318681	4
5.1655407	-2.4452211	2.6232549	3
4.1928335	-2.0287202	2.8711123	4
4.9983035	-3.2259246	1.8865062	4
3.1317292	2.292189	2.033396	3
2.1037571	2.6400222	1.9944886	4
-0.0634142	-0.4152519	2.8906696	3
0.3965454	0.5657957	2.8420351	4
-1.1053991	-0.2855166	3.1627922	4
-6.6330576	-2.274742	-1.8808095	3
-5.6636113	-2.7528642	-1.9989611	4
-8.0191596	1.7374677	0.3248834	3
-8.241336	0.9285282	-0.3617313	4
-8.225272	1.3761285	1.3296199	4
-3.416421	0.9979734	-3.2366549	3
-4.4079944	1.360492	-3.4938534	4
-2.6866461	1.6515336	-3.7122243	4
-0.0351599	2.7525727	-1.4569516	3
0.8070356	2.473336	-2.0773407	4
-0.9418553	2.472879	-1.9772023	4
-3.2867739	-2.7609097	1.0533592	3
-2.2484956	-2.9713125	1.2889149	4
-3.7214197	-2.1941498	1.8686382	4
-0.0468477	4.2457129	-1.1734229	3
-0.9177493	4.5156787	-0.5812864	4
0.8400913	4.5588	-0.6270284	4
-0.0854798	4.8067762	-2.1082509	4
-3.2458147	-0.4212157	-3.7369691	3
-3.9734844	-1.0758763	-3.2732985	4
-3.4006889	-0.4451046	-4.8184475	4
-2.2466702	-0.7838026	-3.529696	4
-4.069217	-4.0470363	0.847756	3
-5.1123432	-3.8245945	0.6465856	4
-3.6664684	-4.6253155	0.017707	4
-4.0212813	-4.6634863	1.7473595	4
-8.8906486	2.9487944	0.0244126	3
-8.7357425	3.2895546	-0.9970756	4
-9.9502946	2.7095327	0.1489073	4
-8.6558848	3.7810325	0.687834	4
0.6604376	-1.2903263	3.9004738	3
0.1999651	-2.2743698	3.9618881	4
1.7033388	-1.4146924	3.6268159	4
0.6203919	-0.8329605	4.8905017	4
5.797393	-3.0424494	3.8728609	3
5.1675377	-3.8295588	4.2933456	4
6.7725113	-3.4727116	3.6483839	4
5.9423647	-2.2790401	4.6348449	4
-6.3317102	-0.2051734	2.9892409	3
-5.3320276	-0.2791008	3.4093074	4
-6.5178847	0.8482618	2.7955832	4
-7.3498922	-0.7430489	3.9844776	3
-8.3613268	-0.6451108	3.5943009	4
-7.1764566	-1.7990099	4.1866294	4
-7.2958757	-0.2044218	4.9337788	4
-3.1758199	2.4694925	1.7880551	3

-4.2042074	2.7843247	1.9343037	4
-0.192464	-2.3799492	-2.3425166	3
0.5365376	-2.5467784	-3.1324373	4
-1.1768907	-2.4586306	-2.7943733	4
-0.0550977	-3.4366395	-1.262808	3
-0.1089254	-4.4264458	-1.7212242	4
0.8838631	-3.3555603	-0.7262322	4
-0.860161	-3.3545828	-0.5430961	4
2.4528483	-2.6637633	-2.2885966	4
4.238076	-3.8039279	-1.8955903	3
5.2320241	-3.6307704	-1.4960336	4
3.7449817	-4.5752297	-1.3062411	4
4.3399759	-4.1674603	-2.9198187	4
3.4504522	2.7099354	-1.4079209	3
4.321826	2.9664464	-0.8156315	4
2.5764985	3.0416835	-0.86152	4
3.5144239	3.3811293	-2.7713847	3
3.5711303	4.4657406	-2.6609637	4
4.3908888	3.0499479	-3.3234108	4
2.6387497	3.1457589	-3.3721128	4
7.0230913	2.4086525	-1.0213137	3
7.7995907	1.7301132	-1.3598656	4
6.2506834	2.3894538	-1.7842052	4
7.5879281	3.8159998	-0.8848501	3
8.0237327	4.1578765	-1.8268328	4
6.8124697	4.5219795	-0.5935569	4
8.3641206	3.8500902	-0.1217972	4
9.1367763	-1.4370895	-1.9625558	3
9.1920171	-0.6361208	-2.6980663	4
10.1345285	-1.5797992	-1.5393789	4
8.862464	-2.3483072	-2.4923218	4
8.4106853	-0.2047257	-0.3518984	4
3.7061063	2.7952832	1.2673083	4
3.7560152	2.5658618	3.392714	3
4.7798518	2.2040101	3.4169497	4
3.766333	3.6388084	3.5928958	4
3.2002574	2.0743511	4.1887553	4
-7.0185272	-2.5574083	-0.9045118	4
-7.5826131	-2.7626158	-2.9657876	3
-7.6984425	-3.8485942	-2.9297521	4
-8.5664796	-2.3118123	-2.8485863	4
-7.2133539	-2.4951238	-3.9545646	4
-2.8277643	2.9202428	0.8650916	4
-2.2984345	2.8873193	2.9558374	3
-2.639854	2.4328007	3.8841461	4
-1.2653136	2.5960967	2.7925679	4
-2.3276419	3.9716844	3.0793354	4

END